NATIONAL ADVISORY COMMITTEE FOR AERONAUTICS

TECHNICAL NOTE 4098

PROPELLANT VAPORIZATION AS A CRITERION FOR ROCKET-ENGINE

DESIGN; CALCULATIONS USING VARIOUS LOG-PROBABILITY

DISTRIBUTIONS OF HEPTANE DROPS

By Richard J. Priem

Lewis Flight Propulsion Laboratory
Cleveland, Ohio

ERRATA

NACA TECHNICAL NOTE 4098

By Richard J. Priem

1957

The following changes should be made to the report:

Figures 3, 4, 5, 7, and 10: The abscissa should be multiplied by 1.30.

Figure 3(a): The ordinate values should be 500, 588, 676, 764, and 852.

Figures 3(e) and 4(c): The ordinate should be divided by 1.30.

Page 5, paragraph 3: Lines 5 and 6 should read "temperatures of all the drops rise to 835° R (corresponding vapor pressure of approximately 118 lb/sq in.); this is the wet-bulb temperature"

Issued 4-18-58

NATIONAL ADVISORY COMMITTEE FOR AERONAUTICS

TECHNICAL NOTE 4098

PROPELLANT VAPORIZATION AS A CRITERION FOR ROCKET-ENGINE

DESIGN; CALCULATIONS USING VARIOUS LOG-PROBABILITY

DISTRIBUTIONS OF HEPTANE DROPS

By Richard J. Priem

SUMMARY

Calculations were made to determine the vaporization rates of fuel drops in a rocket engine for sprays having various log-probability distributions of n-heptane drops. The rates were also calculated for various engine design and operating parameters. The results indicate that a longer chamber is required to obtain a given percent of fuel vaporized for a spray with an increasing geometric standard deviation or an increasing mass-median drop size. The calculations also indicate that a small number of large drops that do not vaporize completely may be responsible for the loss in engine performance. Experimental engine performance results agree with the calculations for a spray having a geometric standard deviation of 2.5 and mass-median drop radii of 70 to 280 microns, depending on the type of injector. The calculations of the percent of fuel vaporized can be correlated with an effective length for various engine design and operating parameters.

INTRODUCTION

Preliminary calculations (ref. 1) for the rate of fuel vaporization in the combustion chamber of a heptane-oxygen rocket engine indicated that propellant vaporization may be a rate-controlling step in the combustion process. The results of these calculations, based on a combustion model in which vaporization of the fuel was rate-controlling, showed how various design and operating parameter changes would effect the vaporization rates of n-heptane drops. The results were limited to one fuel (heptane) and to the assumption that all of the fuel injected into the chamber was of one drop size. It was pointed out that the experimental results agreed with the calculated results except at the high percent of fuel evaporated and percent theoretical performance levels. This difference in experimental and calculated results was explained qualitatively as resulting from a distribution of drop sizes.

The necessity for extending the calculations to consider a distribution of drop sizes is evident, since such results would afford a more realistic correlation between the percent fuel evaporated and actual rocket-engine performance values. This report covers the calculations made at the NACA Lewis laboratory on the vaporization of various log-probability distributions of fuel-drop sizes in a heptane-oxygen rocket combustion chamber.

The results are presented in terms of the combustion-chamber length required to vaporize a given percent of the liquid fuel. The analysis assumes that the fuel is burned as rapidly as it can vaporize. The analysis further assumes one-dimensional steady-state flow. The model and equations of reference 1 are used to determine the velocity, mass, and temperature of the individual drops at various chamber positions.

SYMBOLS

A surface area of drop, sq in.

a constant for number distribution, $\dfrac{600e^{-3(\ln \sigma_g)^2/2}}{M_{g,N}^3 \rho_l \pi \sqrt{2} \ln \sigma_g}$

a' constant for mass distribution, $\dfrac{100}{\sqrt{2\pi} \ln \sigma_g}$

C_D coefficient of drag for spheres, dimensionless

c_p specific heat at constant pressure, Btu/(lb)(°F)

h heat-transfer coefficient, Btu/(sq in.)(sec)(°F)

K coefficient of mass transfer, sec^{-1}

L chamber length, in.

$M_{g,M}$ geometric mean radius for mass distribution, in.

$M_{g,N}$ geometric mean radius for number distribution, $M_{g,M}e^{-3(\ln \sigma_g)^2}$, in.

m_i mass of "i" drop, lb

$m_{i,o}$ mass of "i" drop at beginning of time

N fraction of drops having radii smaller than "r"

n_i number of drops in group of "i" sized drops

p_l vapor pressure of liquid fuel, lb/sq in.

q_v heat-transfer rate to drop, Btu/sec

R   percent of mass in drops smaller than "r"

r   drop radius, in.

T   temperature of gas, °R

T_l temperature of drop, °R

U   velocity difference between gas and drop, in./sec

u   gas velocity, in./sec

u_{fin} final gas velocity, in./sec

v   drop velocity, in./sec

w   vaporization rate of fuel, lb/sec

Z   correction factor for heat transfer, dimensionless

α correction factor for mass transfer, dimensionless

θ time, sec

λ latent heat of vaporization, Btu/lb

ρ_l liquid density, lb/cu in.

ρ_m vapor mixture density, lb/cu in.

σ_g geometric standard deviation, $\dfrac{r \text{ at } R = 84.13}{r \text{ at } R = 50.0}$

METHODS

The fuel injected into the rocket combustion chamber was assumed to be in five groups of drop sizes, which were arbitrarily selected to correspond to a log-probability distribution. Such a distribution is described in reference 2 by the following mathematical expressions:

$$\frac{dN}{dr} = \frac{ae^{-\left[\ln\left(\frac{r}{M_{g,N}}\right)\right]^2 \big/ 2 \ln^2 \sigma_g}}{r} \tag{1}$$

$$\frac{dR}{dr} = \frac{a'e^{-\left[\ln\left(\frac{r}{M_{g,M}}\right)\right]^2 \Big/ 2 \ln^2 \sigma_g}}{r} \qquad (2)$$

where dR/dr is the percent mass and dN/dr is the number of drops in the increment of drop radius Δr for drops with radius r.

Curves for these number and mass distributions (eqs. (1) and (2)) for various geometric standard deviations and for a constant mass-median drop radius of 0.003 inch, as used in the calculations, are shown in figure 1. The accumulated mass-distribution plots of figure 1(a) indicate the variation in slope obtained with the selected values of the standard deviation. The plot for a deviation of 1.0 corresponds to a spray having a single drop size. The mass and number distribution plots of figures 1(b) and (c) indicate that the radius at the distribution peak decreases as the deviation increases.

Because of the difficulty of calculating drop histories for a complete distribution of drop sizes, the five different groups of drop sizes were arbitrarily selected to represent the spray for calculation purposes. These sizes were chosen from the log-probability distribution as those equal to 10, 30, 50, 70, and 90 percent of the mass in drops smaller than the drop radius. The number of drops in each group was so chosen that each group of the five sizes had 20 percent of the total mass. Plots of the distribution obtained by this method are shown in figure 2.

The calculation used the model, the calculation technique, and the following equations of reference 1:

Mass-transfer rate,

$$w = AKp_l\alpha \qquad (3)$$

Heat-transfer rate,

$$q_v = Ah(T - T_l)Z \qquad (4)$$

Drop-heating rate,

$$\frac{dT}{d\theta} = \frac{q_v - w\lambda}{m_l c_{p,l}} \qquad (5)$$

Drop acceleration,

$$\frac{dv}{d\theta} = -\frac{3}{8}\frac{C_D\rho_m U^2}{\rho_l r} \qquad (6)$$

Equations (3) to (6) are explained in greater detail in reference 1.

The gas velocity is obtained by applying the continuity equation for a steady-flow process to obtain

$$\frac{u}{u_{fin}} = 1 - \frac{\sum n_i m_i}{\sum n_i m_{i,o}} \qquad (7)$$

Equation (7) is obtained by integrating equation (12) of reference 1 and summing for all the drops. The gas-velocity ratio is proportional to the fraction of fuel vaporized.

The equations were solved by an iterative procedure on an electronic computer with a linear interpolation. Table I shows the mass-median drop sizes and the geometric-standard-deviation values as well as the values for the design and operating parameters used in the calculations. Physical properties were determined by the equations given in references 3 and 4 for n-heptane.

RESULTS

A detailed example of the calculations for a spray having a mass-median drop radius of 0.003 inch and a standard deviation of 2.30 is shown in figure 3. Droplet temperatures for each drop size at various positions in the chamber are shown in figure 3(a). The calculated temperatures of all of the drops rise to 880° R (corresponding vapor pressure of approximately 180 lb/sq in.); this is the wet-bulb temperature of the fuel at the conditions specified. The smallest drops attain the wet-bulb temperature in a much shorter chamber length than the large drops. It will be seen later in the report that the smallest drop is completely vaporized in $1\frac{1}{2}$ inches; at this point, the large drop has attained a temperature of only 750° R. Because of this large difference in the distance required to attain the wet-bulb temperature, it is felt that including the heating period of the drops is important.

The gas and drop velocity curves are shown in figure 3(b). Initially the gas velocity increases rapidly; and, in an inch of chamber length, the slope begins to decrease because the small drops are substantially vaporized and the surface area of the larger drops is decreasing. The drop velocities first decrease because they exceed the velocity of the slow moving gas; this decrease is greatest for the smallest drops. A minimum drop velocity is reached when the gas velocity equals the drop velocity. After the minimum point the gas velocity is greater than the drop velocity, and therefore the gas accelerates the drops to higher velocities. The small drops attain a high velocity much faster than the larger drops; thus a mixing effect occurs because of the relative motion of the drops.

The percent-mass-vaporized curves (fig. 3(c)) start out with a high slope on the log-log plot. At the end of the lifetime of each drop, the slope of the percent-mass-vaporized curves decreases because of the decrease in drop surface area. The curves show that, within 2 inches of length, the small drops are almost completely vaporized but only 3 percent of the large drops are vaporized. The average curve, which is the percent of the total mass vaporized, is not as steep as any of the individual curves and crosses the curves for the three intermediate drop-size groups. The inflection point in the curves of the two small-drop-size groups occurs when the gas velocity and drop velocity are equal; this produces a Reynolds number of zero and a small Nusselt number.

The percent-mass-unvaporized curves are shown in figure 3(d). This plot produces better resolution in the 90- to 99-percent-vaporized region. This curve shows that the large drops in the distribution obviously limit the mass fraction of fuel that can be burned within a given rocket-engine length. For the conditions shown, 6 percent of the fuel is unvaporized in 10 inches and therefore is not available to burn in a chamber of that length, although the small drops are completely vaporized in 10 inches.

The curve showing the total vaporization rate per unit length (fig. 3(e)) is similar to those curves shown in reference 1 for single drops, with two peak points and a minimum point in each curve. The minimum point occurs when the gas velocity is equal to the droplet velocities, which produces a Reynolds number of zero and a small Nusselt number. The vaporization rate is initially low because the temperature of the fuel is below the wet-bulb temperature. At the end of the chamber, the rate is also low because of the small surface area of the drops and the high drop velocity. The peak point in the calculated vaporization-rate curve occurs at about 1/4-inch length. Since only 94 percent of the mass is vaporized in 10 inches, a long chamber would be required to attain complete vaporization even with a high vaporization rate close to the injector.

Geometric Standard Deviation

The effect of a change in the geometric standard deviation (change in distribution of drop sizes) is shown in figure 4. In the low percent-mass-vaporized region (fig. 4(a)) little difference exists between a standard deviation of 1.00 and 1.54. However, changes from 1.54 to 2.30 and 3.60 in the standard deviation greatly increase the amount of fuel vaporized near the injector because of the large number of small drops in a normal distribution having a large standard deviation, as shown in figure 1(c). The curves all cross at about 58 percent of the mass vaporized.

The high percent-mass-vaporized region is better shown in figure 4(b). The percent-mass-unvaporized curves show that, the larger the geometric

standard deviation, the longer the chamber required to vaporize a given percentage of the mass. A deviation of 3.60 requires a chamber ten times as long as a deviation of 1.00 (single drop) to vaporize 99 percent of the fuel.

The vaporization-rate curve (fig. 4(c)) shows that, as the standard deviation increases, the first peak in the vaporization-rate curve increases considerably and shifts to shorter distances. As pointed out previously, this is due to the larger number of small drops with larger standard deviations.

Mass-Median Drop Size

The effect of a change in the initial mass-median drop size from 0.001 to 0.009 inch (25 to 225 microns) in diameter is shown in figure 5. As expected and shown for single drops in reference 1, the curves indicate that the smaller median sizes vaporize in a shorter chamber. The percent-mass-vaporized and percent-mass-unvaporized curves have about the same shape for all sizes. This shift in the curves produced by a change in the median size is about the same as that produced for single drops, as shown in reference 1.

Variation in Group Size

The selection of the five drop sizes chosen to represent the normal distribution in the calculations was admittedly arbitrary. For this reason a comparison was made by performing identical calculations with five different drop sizes representing the same distribution. The five groups used in the two cases investigated are shown in figure 6. As can be seen by the results shown in figure 7, there is little difference between these two cases. Consequently, it is felt that the five drop sizes selected in case A and used in most of the calculations were representative of an actual spray. Undoubtedly, if more groups had been used to represent the actual spray, the results would have been slightly different; this minor difference would not appear to justify a more complicated calculation procedure.

Correlation of Results

An attempt was made to fit the results obtained for the conditions listed in table I to a single curve, usable for engine design. The results of the calculations for a distribution having a standard deviation of 1.54 were plotted (fig. 8) with the correction factor on length obtained in reference 1. This correction factor was obtained from a cross plot of the length required to vaporize 90 percent of the mass of single drops.

As in reference 1, the spread in the length for a given percent vaporized was greatest in the low percent-vaporized region. The variation in the position of the inflection point produced most of the spread. The calculated percent of fuel vaporized can be correlated with an effective chamber length obtained by multiplying the chamber length by

$$\frac{P^{0.55} u_{fin}^{0.25} T_{l,0}^{0.25}}{M_{g,M,0}^{1.45} V_0^{0.75}}$$

A plot of the percent-mass-unvaporized as a function of the effective chamber length gave almost a single curve for sprays having a particular standard deviation.

The results were further correlated for all deviations in figure 9 by using average curves. The effective length required to obtain 40, 60, 80, 90, 95, and 99 percent-mass-vaporized data are shown in figure 9 for sprays with various standard deviations; this permits interpolation between the standard deviations plotted.

DISCUSSION OF RESULTS

A comparison of the experimental data presented in reference 5 and the correlated curves of this report is included in figure 10. Results for three different injector types are shown, and the mass-median drop size used for each injector is listed. The results of figure 10(b) show that the experimental results follow the calculated curves for a standard deviation of about 2.5 with a mass-median drop radius of approximately 280 microns for a parallel-jet injector, 150 microns for a parallel-sheet injector, and 70 microns for a triplet injector. Each injector is described in detail in reference 5. The curves indicate a reasonable correlation between the experimental percent of theoretical characteristic exhaust velocity (performance) of a rocket engine and the percent of fuel vaporized in various chamber lengths if a drop-size distribution is used in the calculations.

The loss in performance of an engine can be explained as due to unvaporized fuel. The fuel that does not vaporize is the fuel originally contained in the larger drops, as shown in figure 3(d). While the number of large drops is a very small fraction of the drops in the spray (fig. 1(c)), the amount of mass in the large drops is appreciable. This fact indicates that rocket performance can be increased by minimizing the large drops.

The standard deviation estimated for the experimental sprays on the basis of the vaporization hypothesis was approximately 2.5. This value is somewhat larger than the value of about 1.5 reported in reference 6.

However, the sprays of reference 6 were produced under turbojet and ram-jet conditions by spraying into a high-velocity gas stream, which could produce sprays with different standard deviations.

Experimental results are needed to determine the characteristics of sprays formed in rocket engines with various injectors. Calculations also are needed for other propellants in order to make the results more general. The results indicate that eliminating the large drops in the sprays would be very beneficial and that work should be undertaken to accomplish this purpose. Additional work is also needed in checking the applicability of the empirical correction factors used in the correlation over a wide range of conditions, as was done for the effect of fuel temperature in reference 7.

SUMMARY OF RESULTS

Calculations were made to determine the vaporization rates of fuel drops in a rocket engine for sprays having various log-probability distributions of n-heptane drops and mass-median drop sizes and for various engine design and operating parameters in order to show how these variables would affect the vaporization rate and chamber length required to vaporize the drops. The results are correlated with an effective length and are compared with experimental results. The experimental results correlate with the calculations for sprays having a geometric standard deviation of 2.5 and mass-median drop radii of 70 to 280 microns, depending on the injector type. A small number of large drops that do not completely vaporize may be responsible for the loss in engine performance. The calculations have shown quantitatively that the chamber length required to vaporize a given high percentage of fuel increases with increasing geometric standard deviation and mass-median drop radius.

Lewis Flight Propulsion Laboratory
    National Advisory Committee for Aeronautics
        Cleveland, Ohio, August 8, 1957

REFERENCES

1. Priem, Richard J.: Propellant Vaporization as a Criterion for Rocket Engine Design; Calculations of Chamber Length to Vaporize a Single n-Heptane Drop. NACA TN 3985, 1957.

2. Bevans, Rowland S.: Mathematical Expressions for Drop Size Distributions in Sprays. Conf. on Fuel Sprays, Univ. of Mich., March 30-31, 1949.

3. Priem, Richard Jerome: Vaporization of Fuel Drops Including the
      Heating-Up Period. Ph.D. Thesis, Univ. Wis., 1955.

4. El Wakil, M. M., Priem, R. J., Brikowski, H. J., Myers, P. S., and
      Uyehara, O. A.: Experimental and Calculated Temperature and Mass
      Histories of Vaporizing Fuel Drops. NACA TN 3490, 1956.

5. Heidmann, M. F., and Auble, C. M.: Injection Principles from Combustion
      Studies in a 200-Pound-Thrust Rocket Engine Using Liquid Oxygen and
      Heptane. NACA RM E55C22, 1955.

6. Ingebo, Robert D.: Vaporization Rates and Drag Coefficients for Iso-
      octane Sprays in Turbulent Air Streams. NACA TN 3265, 1954.

7. Heidmann, M. F.: Propellant Vaporization as a Criterion for Rocket-
      Engine Design; Experimental Effect of Fuel Temperatures on Liquid-
      Oxygen - Heptane Performance. NACA RM E57E03, 1957.

4534

TABLE I. - RANGE OF CONDITIONS USED FOR CALCULATIONS

[Gas temp., 5000° R.]

Mass-mean drop radius, in.	Geometric standard deviation	Initial drop temperature, °F	Initial drop velocity, in./sec	Final gas velocity, in./sec	Chamber pressure lb/sq in.
0.001	1.54	500	1200	9,600	300
0.003	1.00	500	1200	9,600	300
	1.25	500	1200	9,600	300
	1.54	400	1200	9,600	300
		500	600	9,600	300
				19,200	300
			1200	2,400	300
				9,600	150
					300
					600
				19,200	300
			2400	9,600	300
		700	1200	9,600	300
	2.30	500	1200	9,600	300
	3.60	500	1200	9,600	300
0.009	1.54	500	1200	9,600	300

Drop radius, in.

.03
.02
.01
.008
.006
.004
.002
.001
.0008
.0006
.0004
.0003

Geometric
standard
deviation,
σ_g

1.0

1.25

1.54

2.3

3.6

$M_{g,M}$

84.13

.01 .05 .1 .5 1 2 5 10 20 50 60 70 80 90 95 98 99 99.8 99.9 99.99

Percent mass in drops smaller than r, R
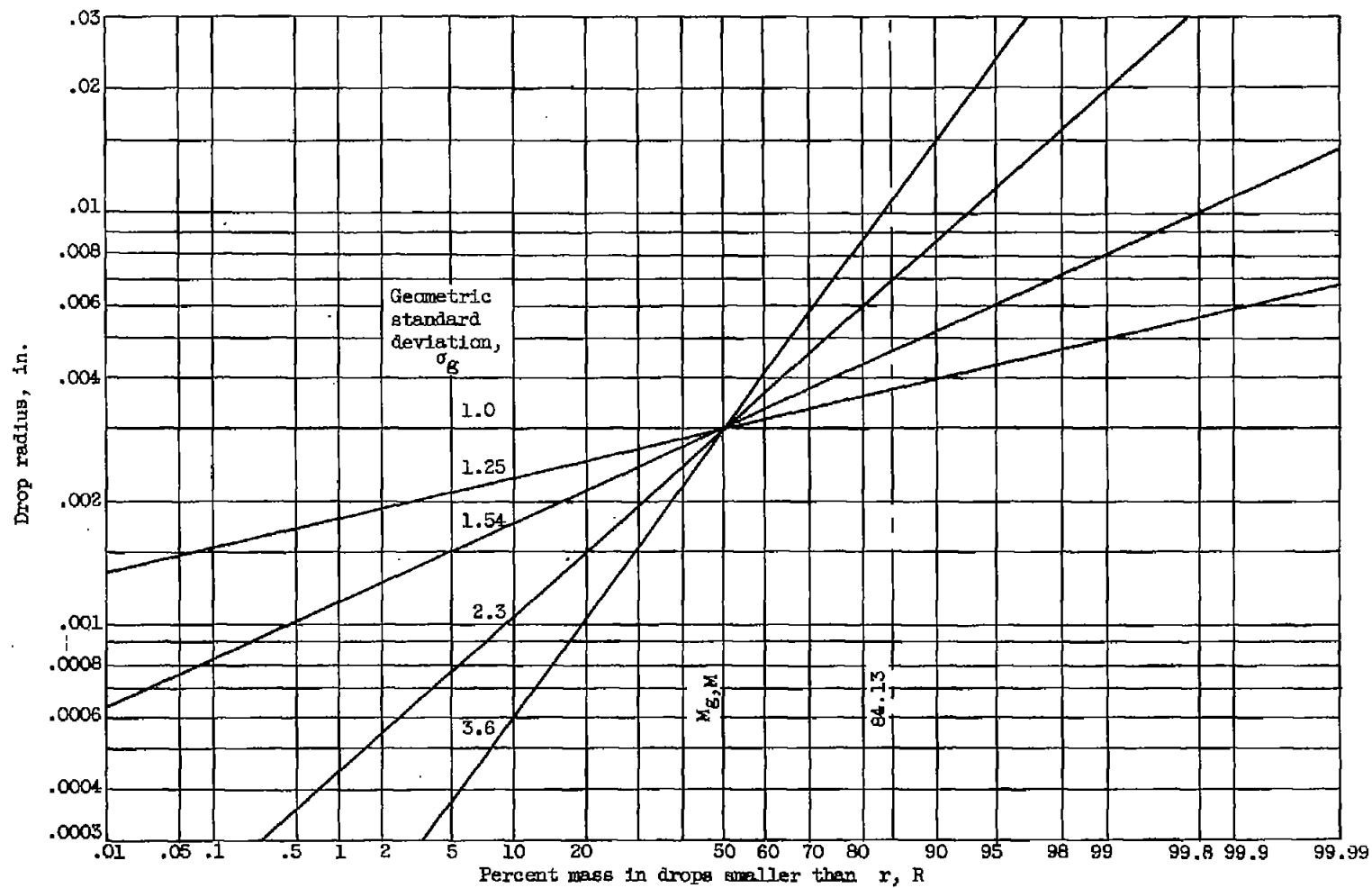
(a) Accumulated drop-mass distribution. $R = \frac{1}{2} \pm \dfrac{\Gamma \log \left(\dfrac{r}{M_{g,M}}\right)^{1/2}}{2\Gamma_{1/2}}$

Figure 1. - Mass and number distribution curves. Mass-median radius, 0.003 inch.
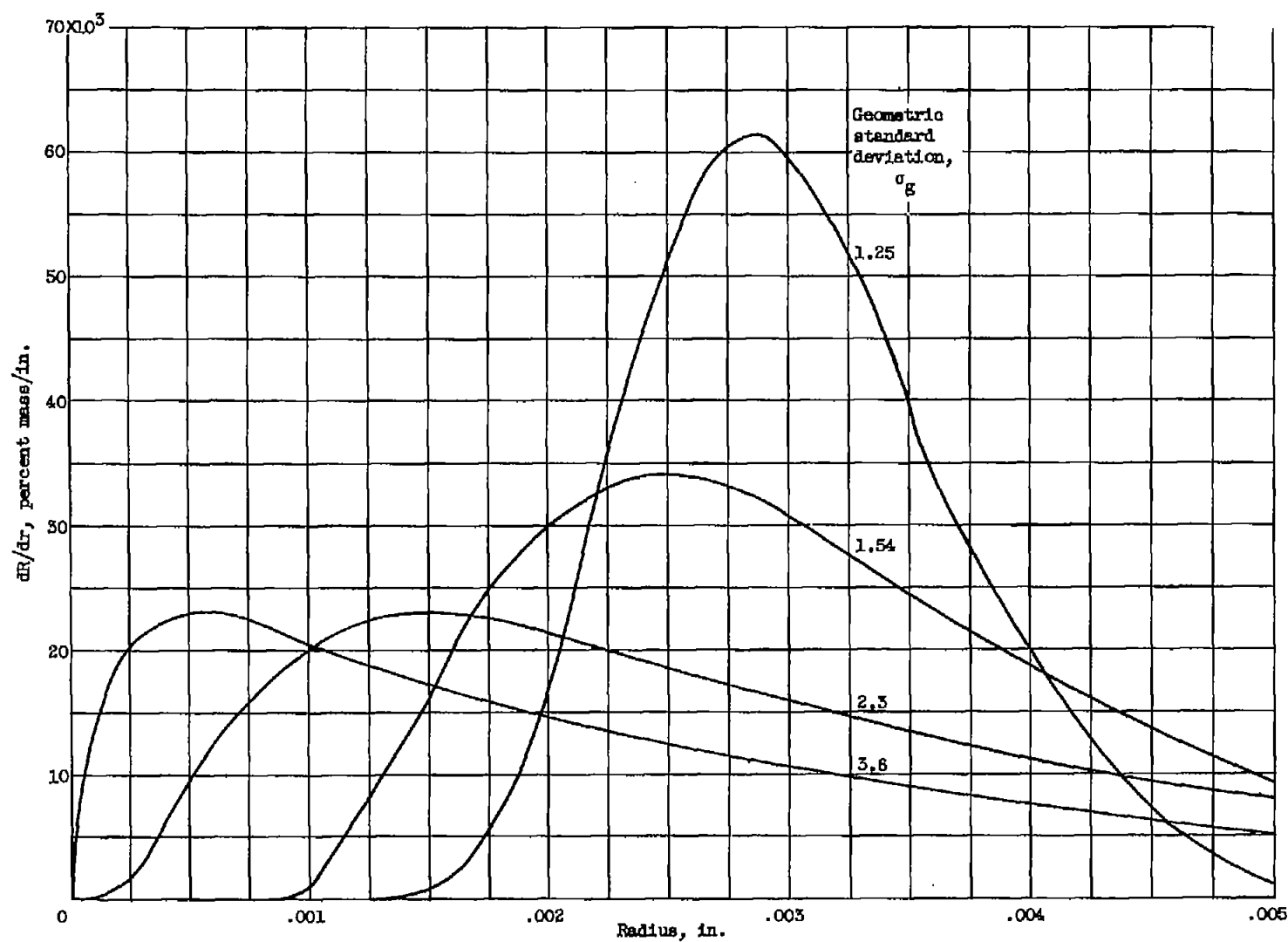
(b) Drop-mass distribution.

Figure 1. - Continued. Mass and number distribution curves. Mass-median radius, 0.003 inch.
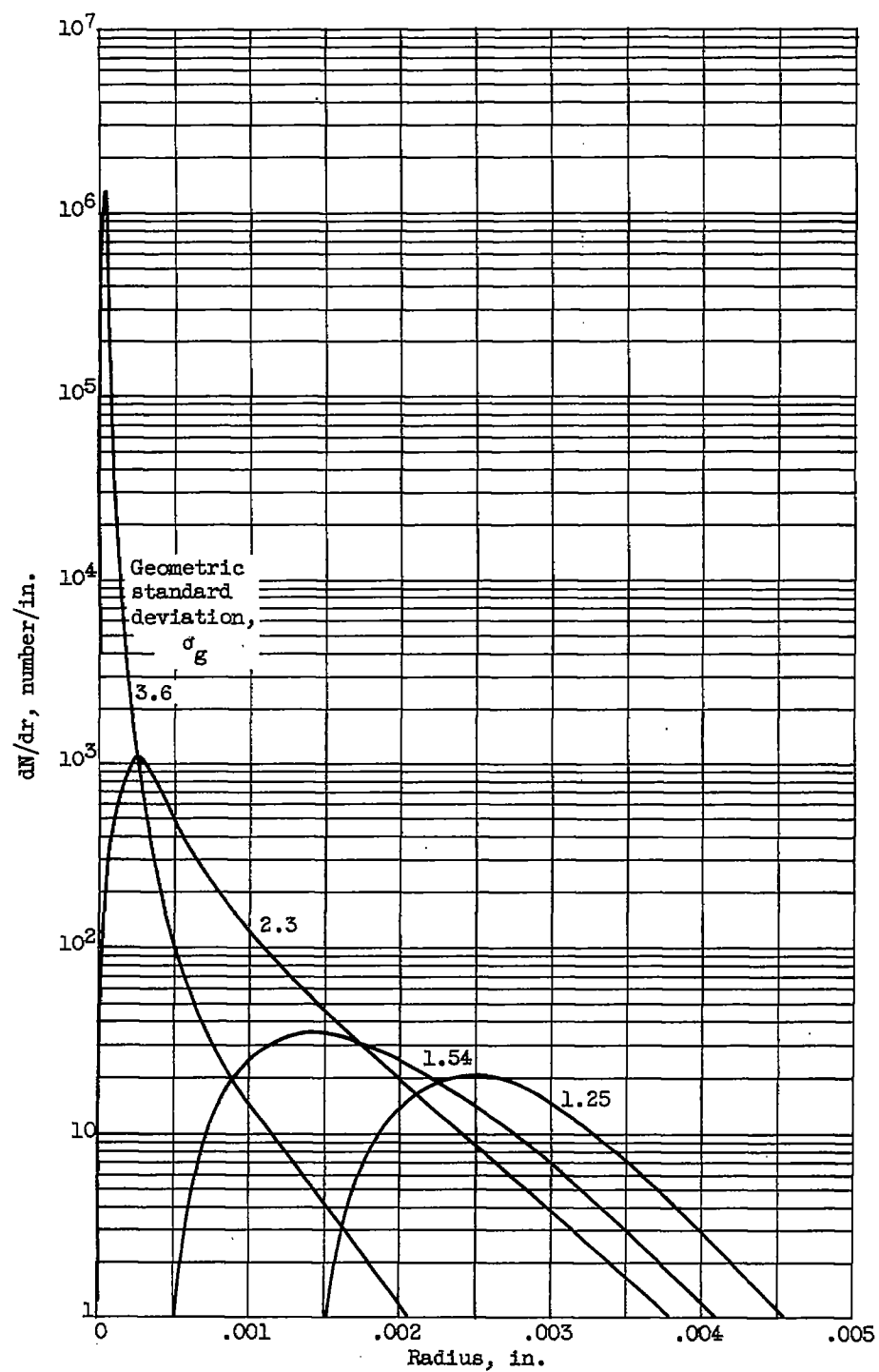
(c) Drop-size distribution.

Figure 1. - Concluded. Mass and number distribution curves.
Mass-median radius, 0.003 inch.
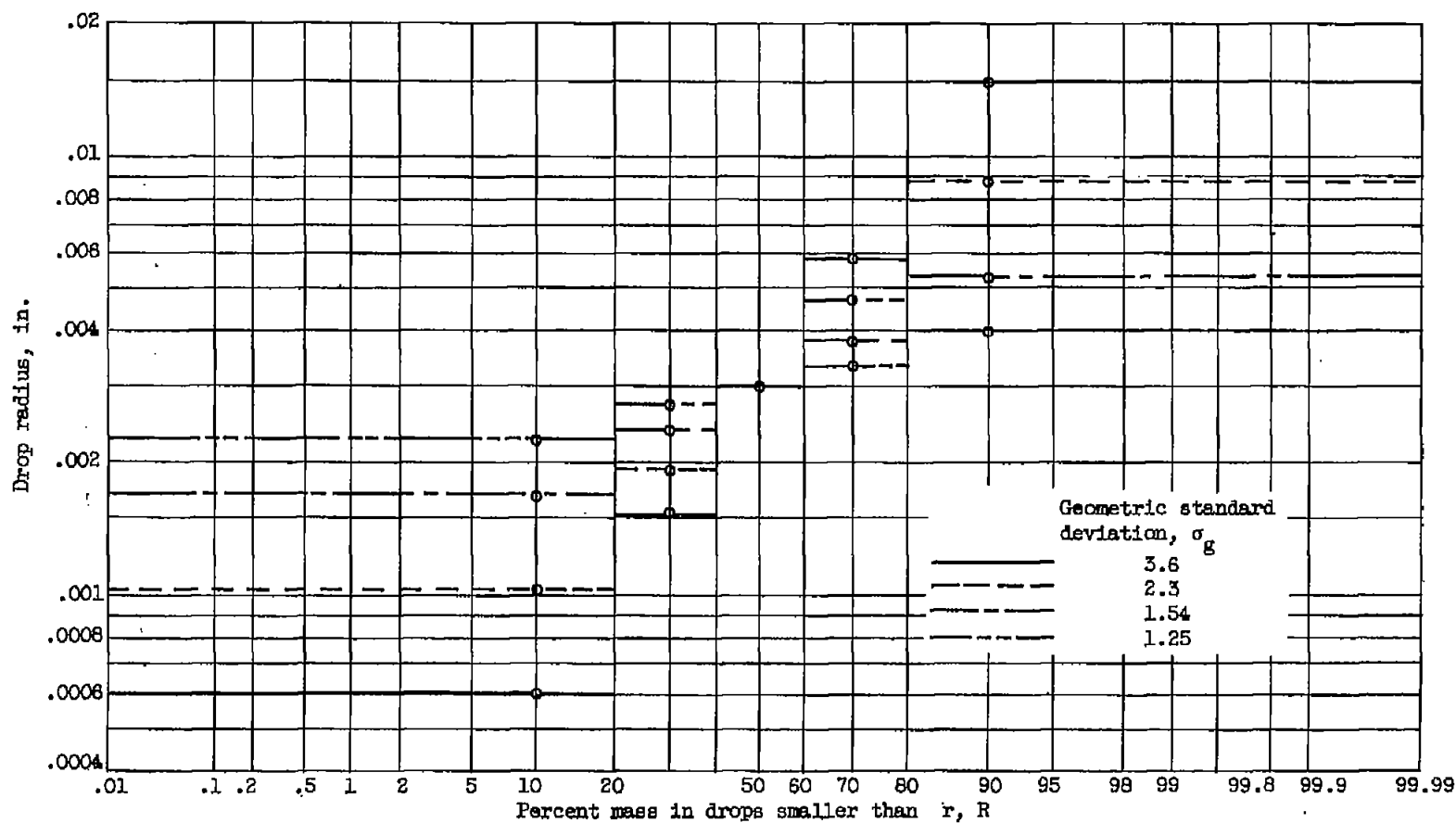
Figure 2. - Accumulated drop-mass distributions used in calculations. Mass-median radius, 0.003 inch.
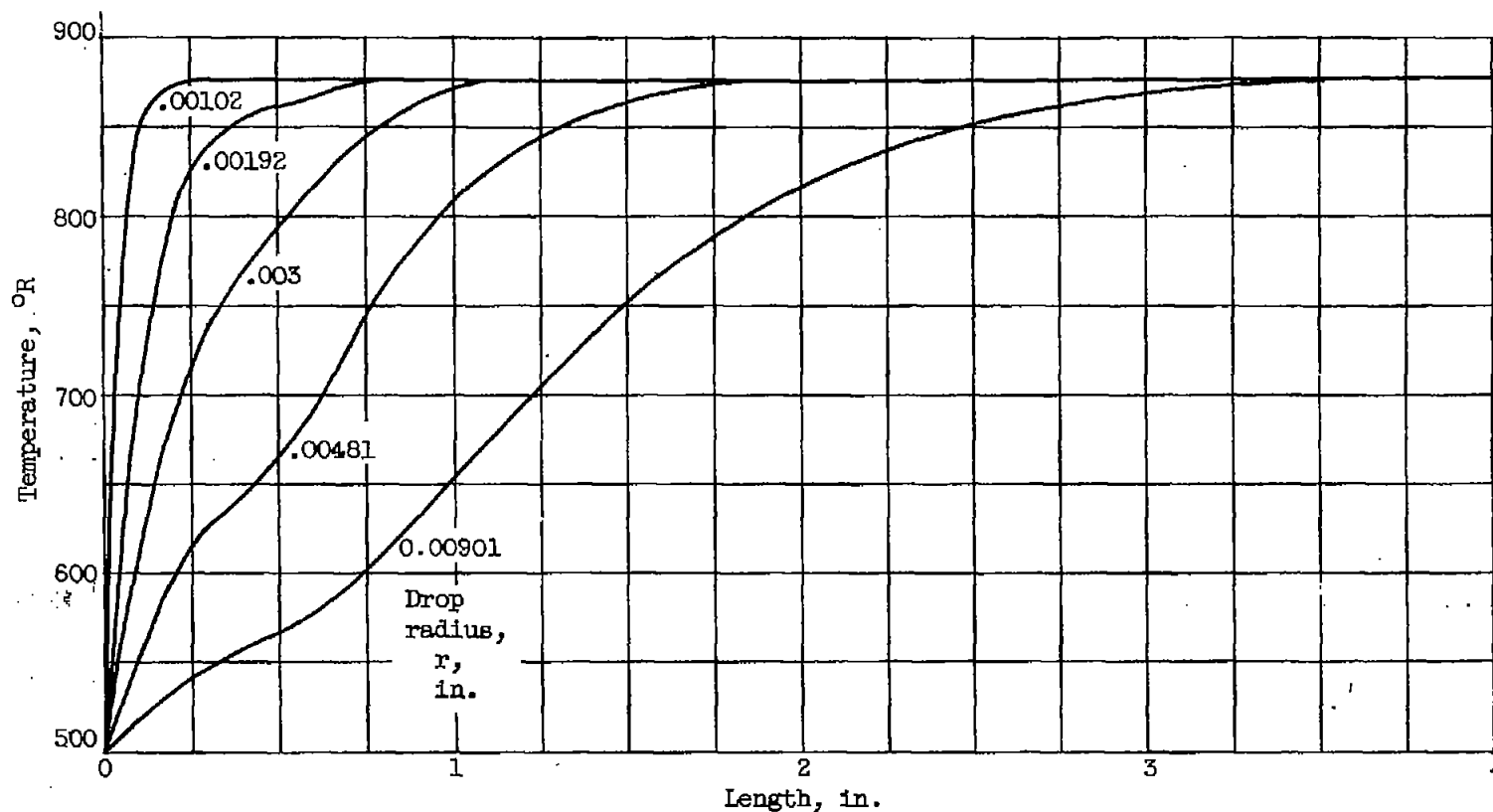
(a) Drop temperatures.

Figure 3. - Typical drop histories. Mass-median drop radius, 0.003 inch; standard deviation, 2.30; initial drop temperature, 500° R; initial drop velocity, 1200 inches per second; final gas velocity, 9600 inches per second; gas temperature, 5000° R; chamber pressure, 300 pounds per square inch absolute.
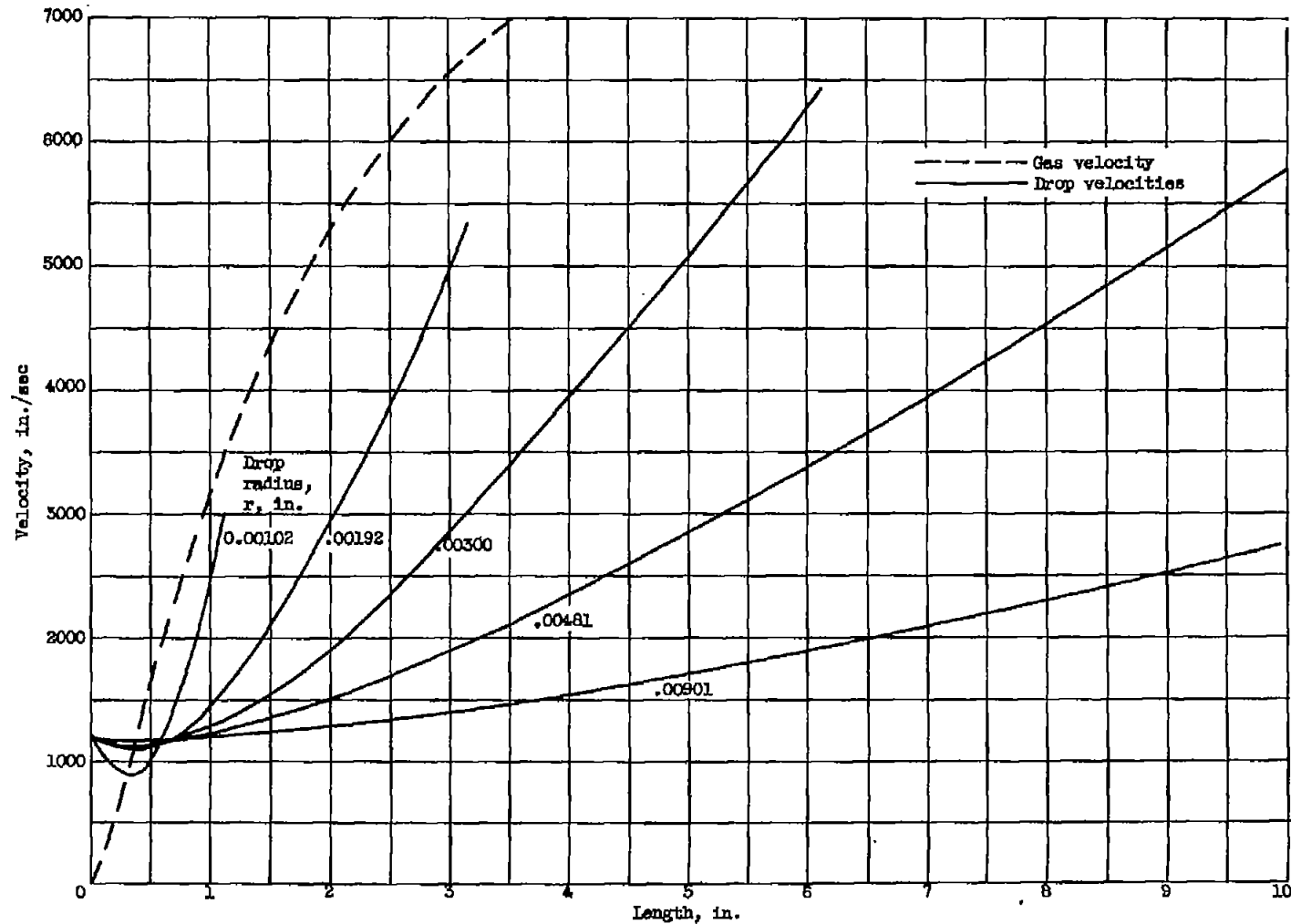
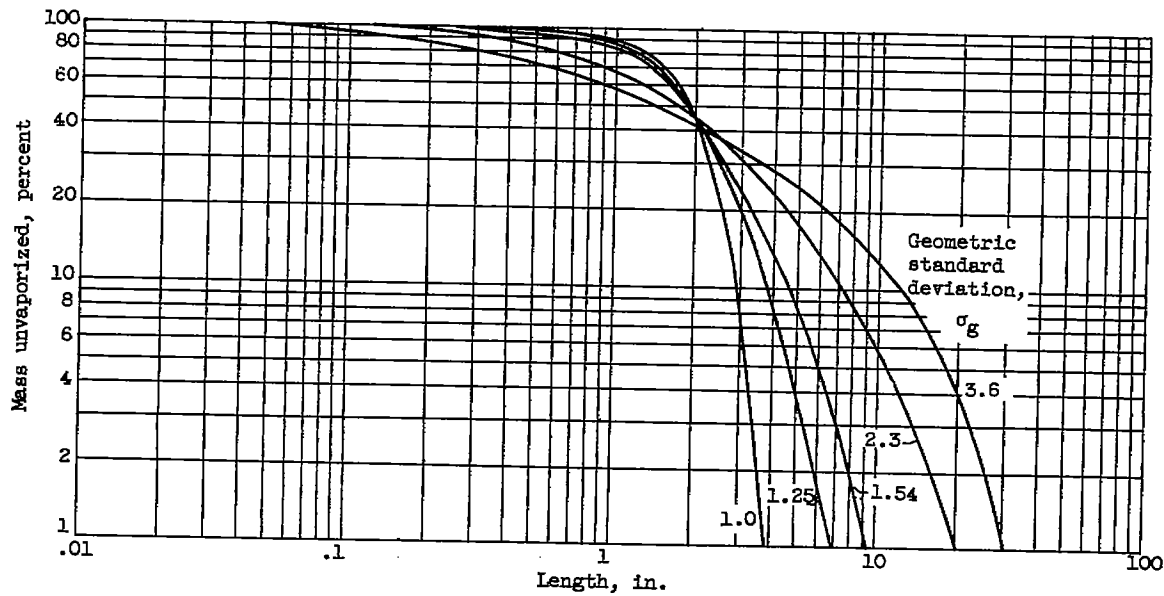(b) Gas velocity and drop velocities.

Figure 3. - Continued. Typical drop histories. Mass-median drop radius, 0.003 inch; standard deviation, 2.30; initial drop temperature, 500° R; initial drop velocity, 1200 inches per second; final gas velocity, 9600 inches per second; gas temperature, 5000° R; chamber pressure, 300 pounds per square inch absolute.
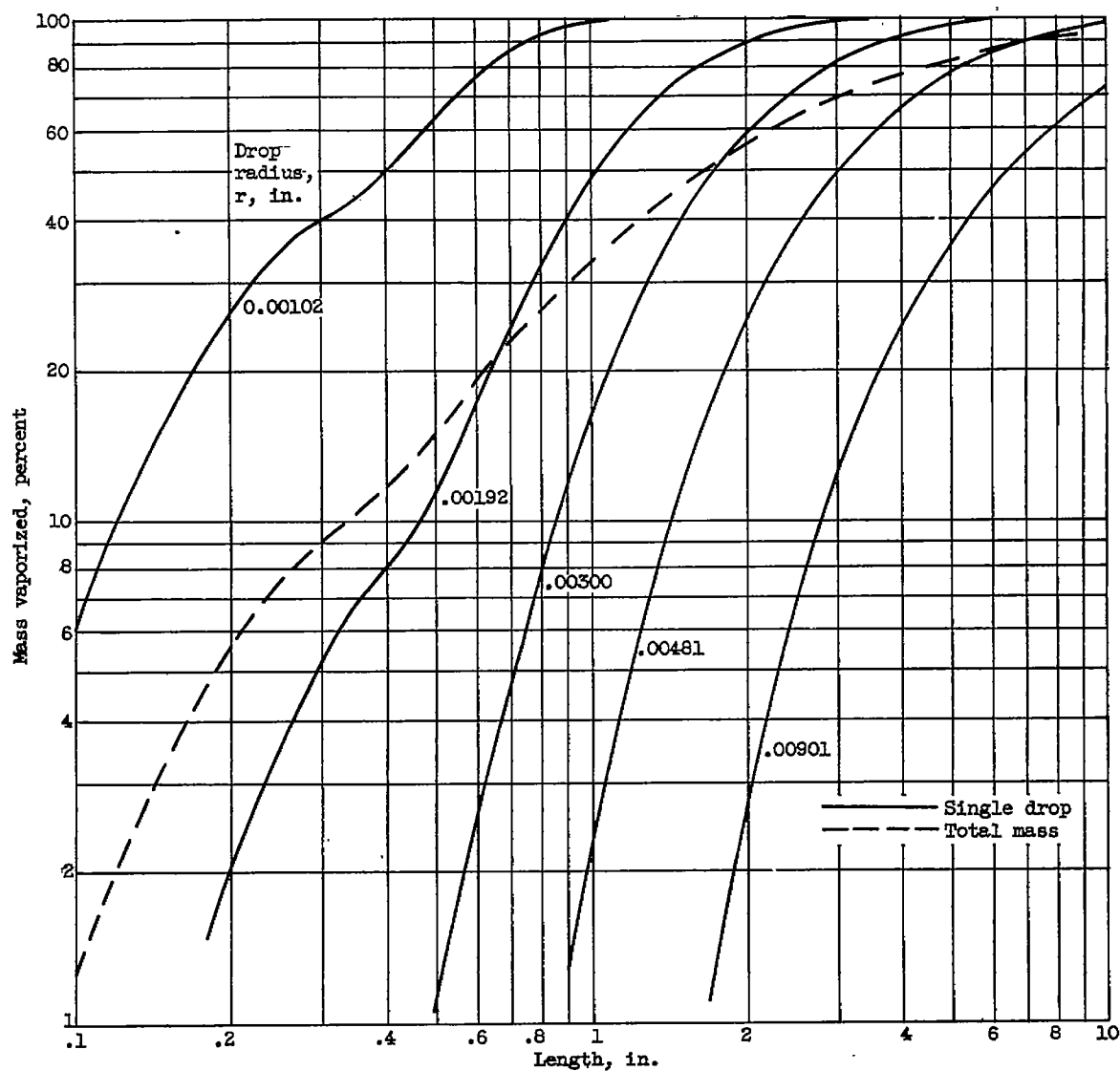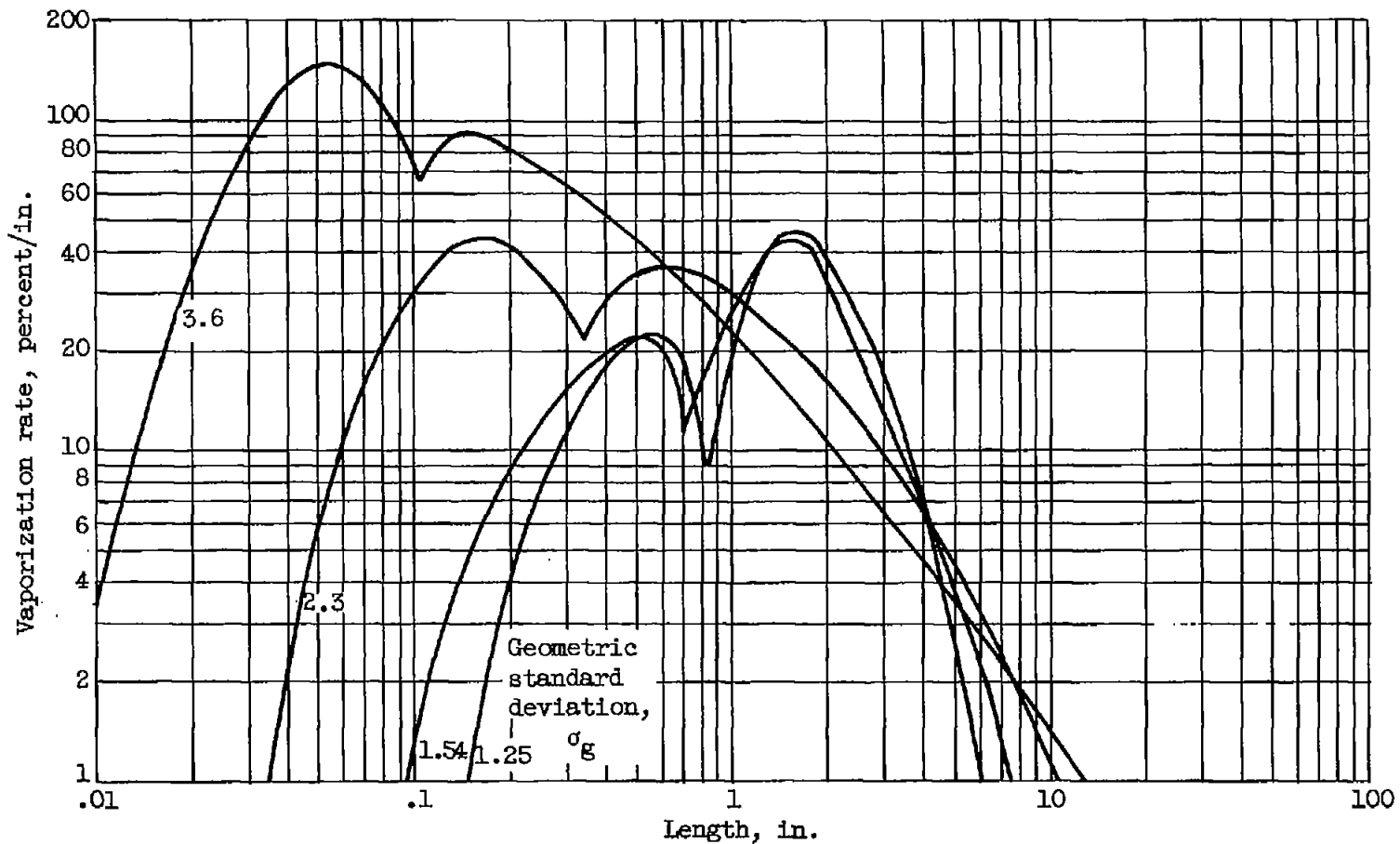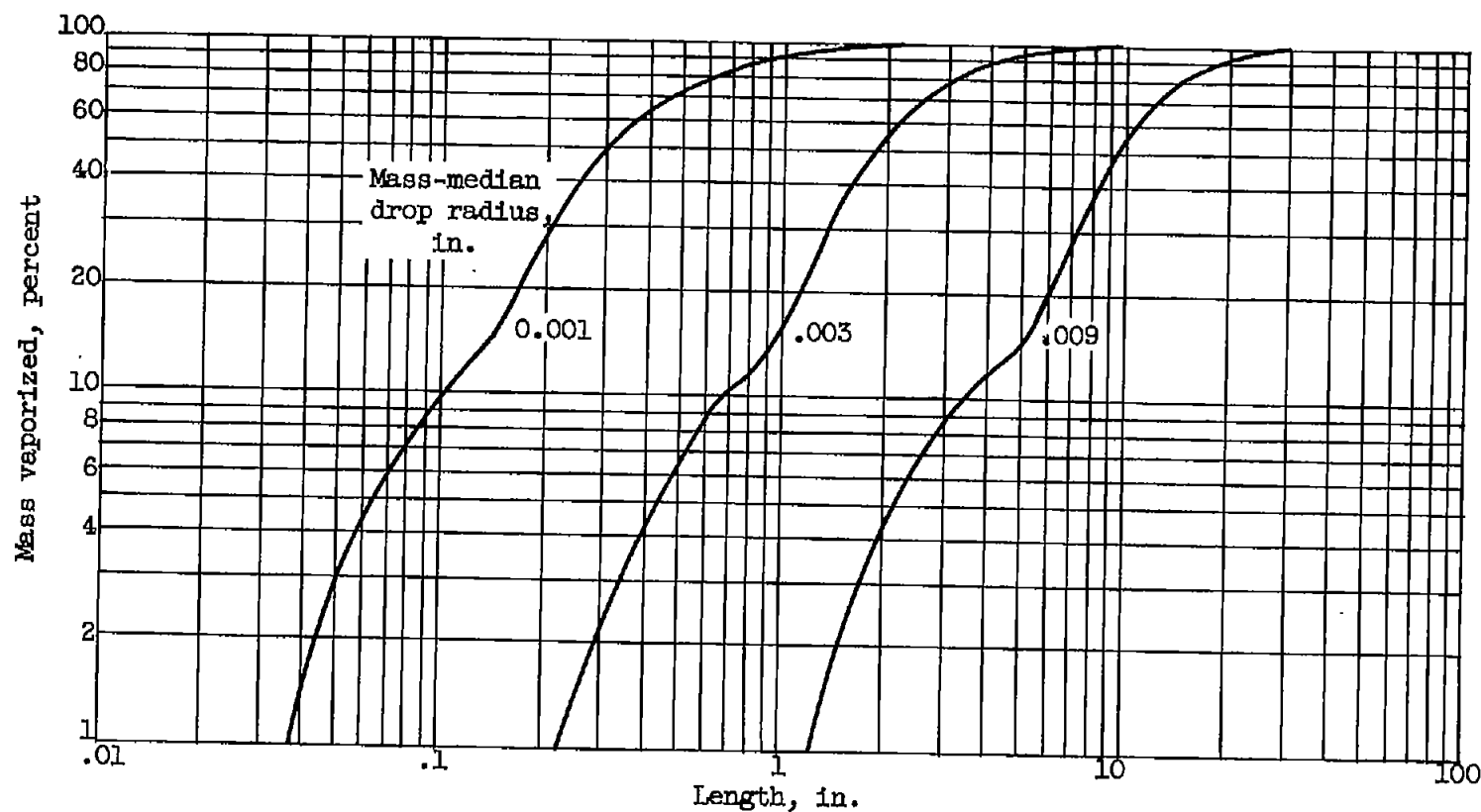
(c) Mass vaporized.

Figure 3. - Continued. Typical drop histories. Mass-median drop radius, 0.003 inch; standard deviation, 2.30; initial drop temperature, 500° R; initial drop velocity, 1200 inches per second; final gas velocity, 9600 inches per second; gas temperature, 5000° R; chamber pressure, 300 pounds per square inch absolute.
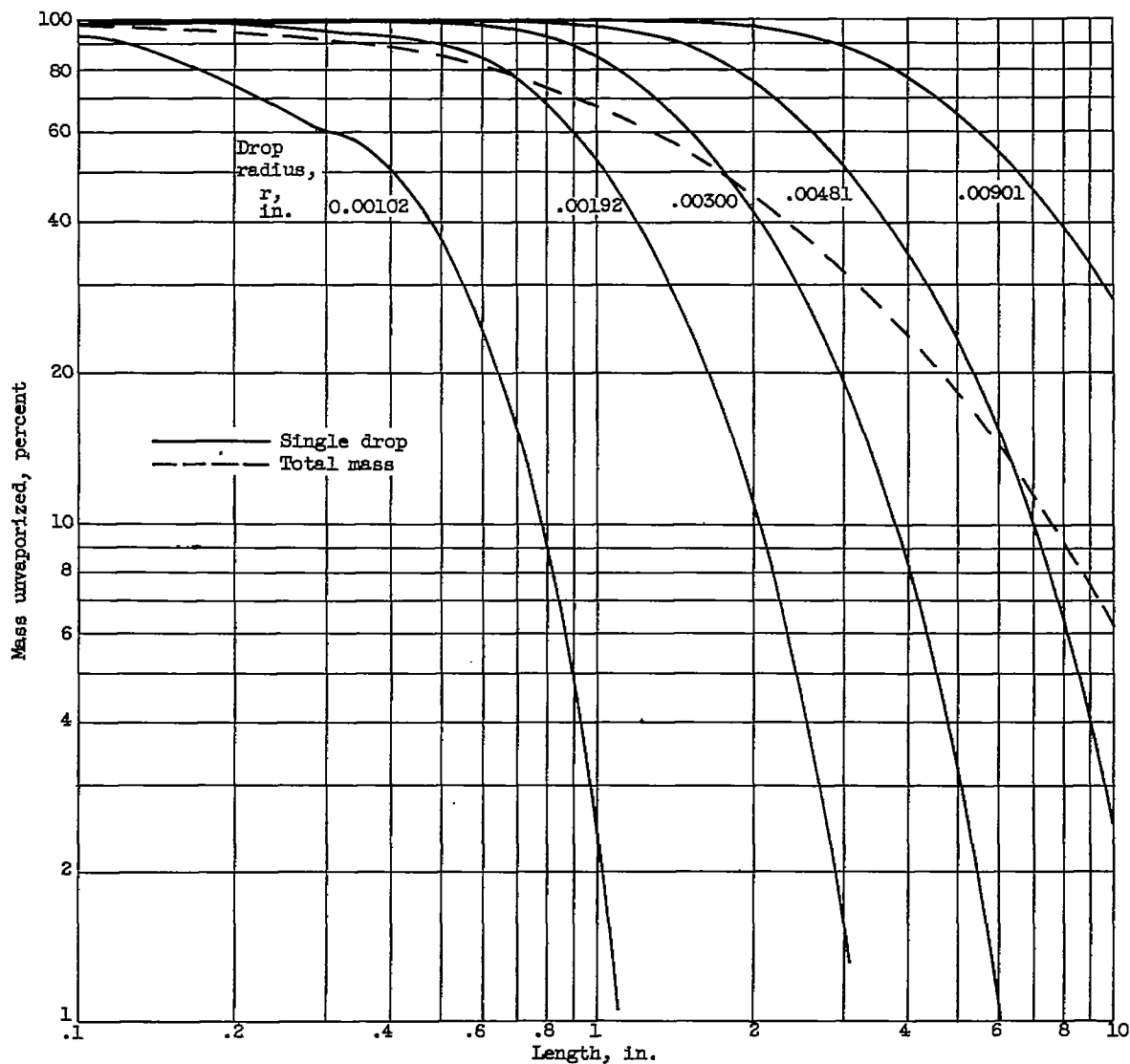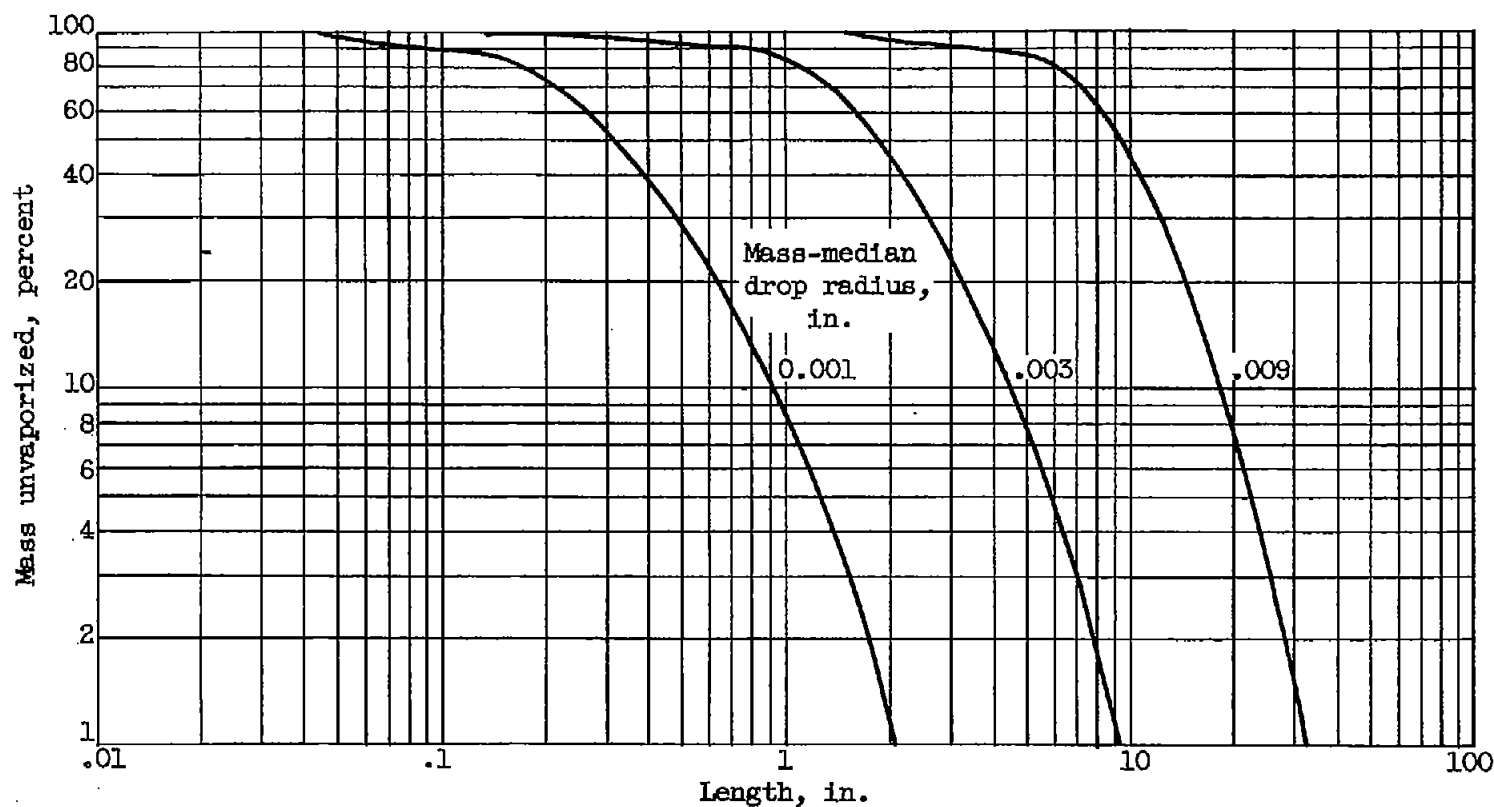
(d) Mass unvaporized.

Figure 3. - Continued. Typical drop histories. Mass-median drop radius, 0.003 inch; standard deviation, 2.30; initial drop temperature, 500° R; initial drop velocity, 1200 inches per second; final gas velocity, 9600 inches per second; gas temperature, 5000° R; chamber pressure, 300 pounds per square inch absolute.
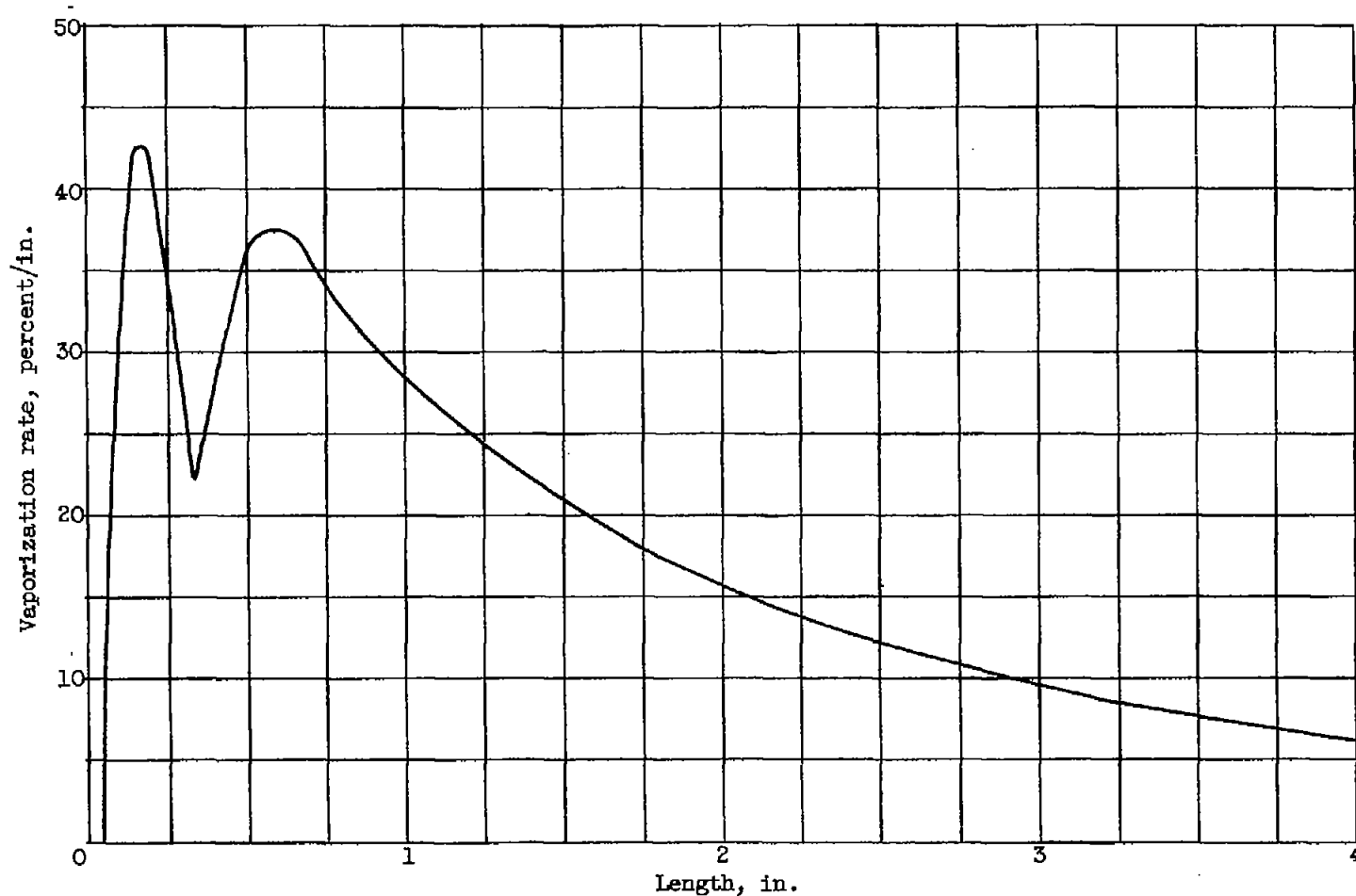
(e) Total vaporization rate.

Figure 3. - Concluded. Typical drop histories. Mass-median drop radius, 0.003 inch; standard
deviation, 2.30; initial drop temperature, 500° R; initial drop velocity, 1200 inches per
second; final gas velocity, 9600 inches per second; gas temperature, 5000° R; chamber pres-
sure, 300 pounds per square inch absolute.

4534
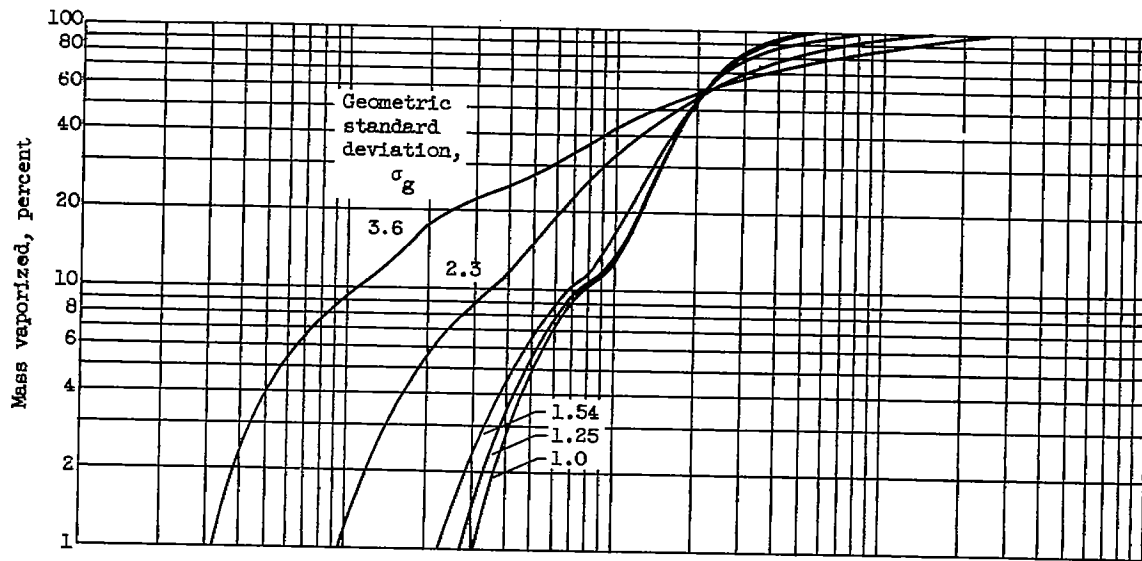
(a) Mass vaporized.

(b) Mass unvaporized.

Figure 4. - Effect of geometric standard deviation. Mass-median drop radius, 0.003 inch; initial drop temperature, 500° R; initial drop velocity, 1200 inches per second; final gas velocity, 9600 inches per second; gas temperature, 5000° R; chamber pressure, 300 pounds per square inch absolute.

(c) Vaporization rate.

Figure 4. - Concluded. Effect of geometric standard deviation. Mass-median drop radius, 0.003 inch; initial drop temperature, 500° R; initial drop velocity, 1200 inches per second; final gas velocity, 9600 inches per second; gas temperature, 5000° R; chamber pressure, 300 pounds per square inch absolute.
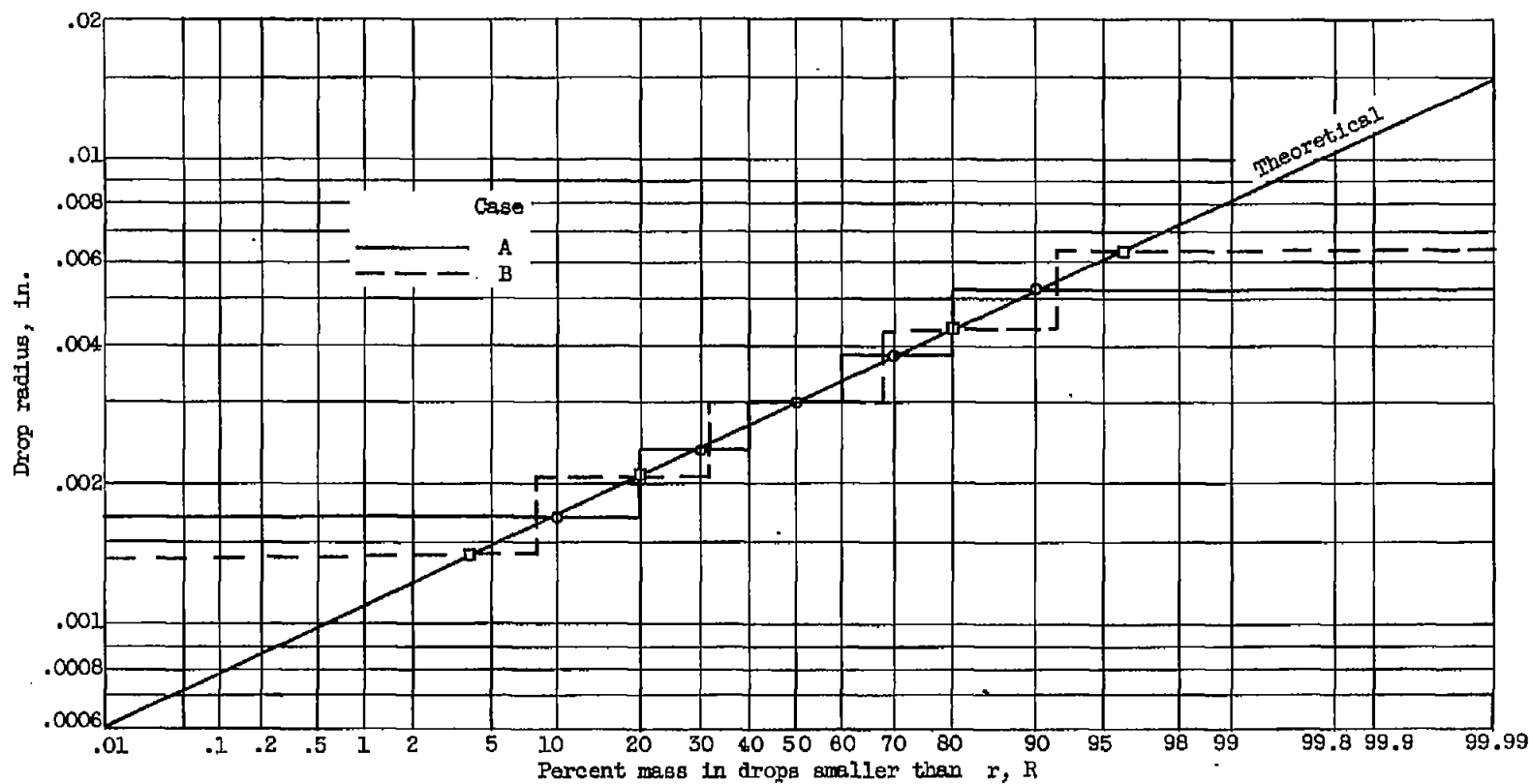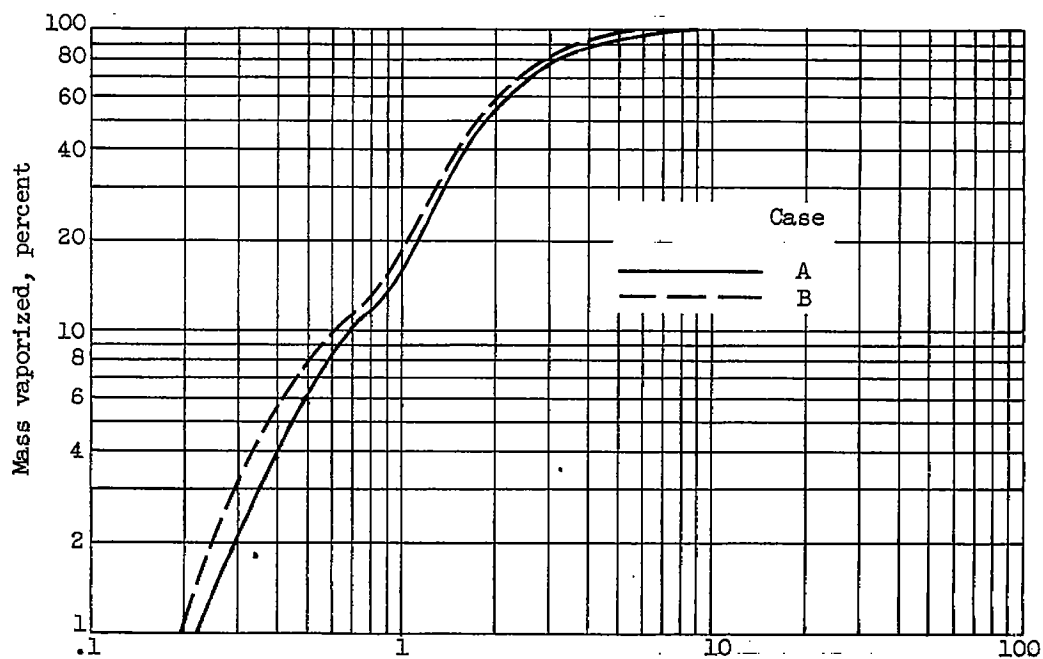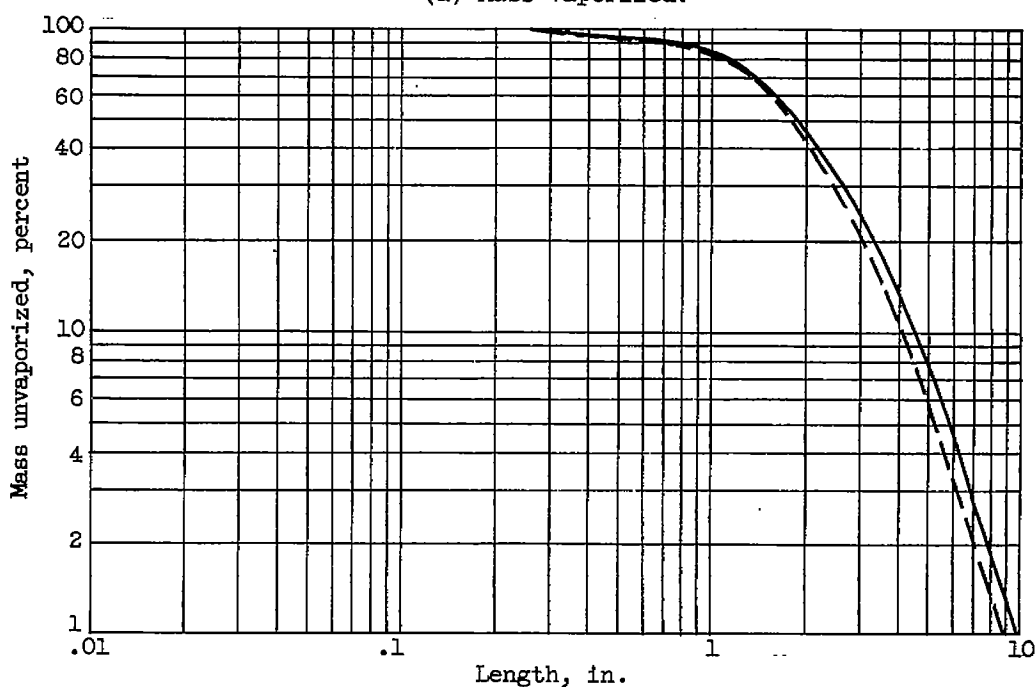
(a) Mass vaporized.

Figure 5. - Effect of mass-median drop size. Geometric standard deviation, 1.54; initial drop temperature, 500° R; initial drop velocity, 1200 inches per second; final gas velocity, 9600 inches per second; gas temperature, 5000° R; chamber pressure, 300 pounds per square inch absolute.

(b) Mass unvaporized.

Figure 5. - Concluded. Effect of mass-median drop size. Geometric standard deviation, 1.54; initial drop temperature, 500° R; initial drop velocity, 1200 inches per second; final gas velocity, 9600 inches per second; gas temperature, 5000° R; chamber pressure, 300 pounds per square inch absolute.

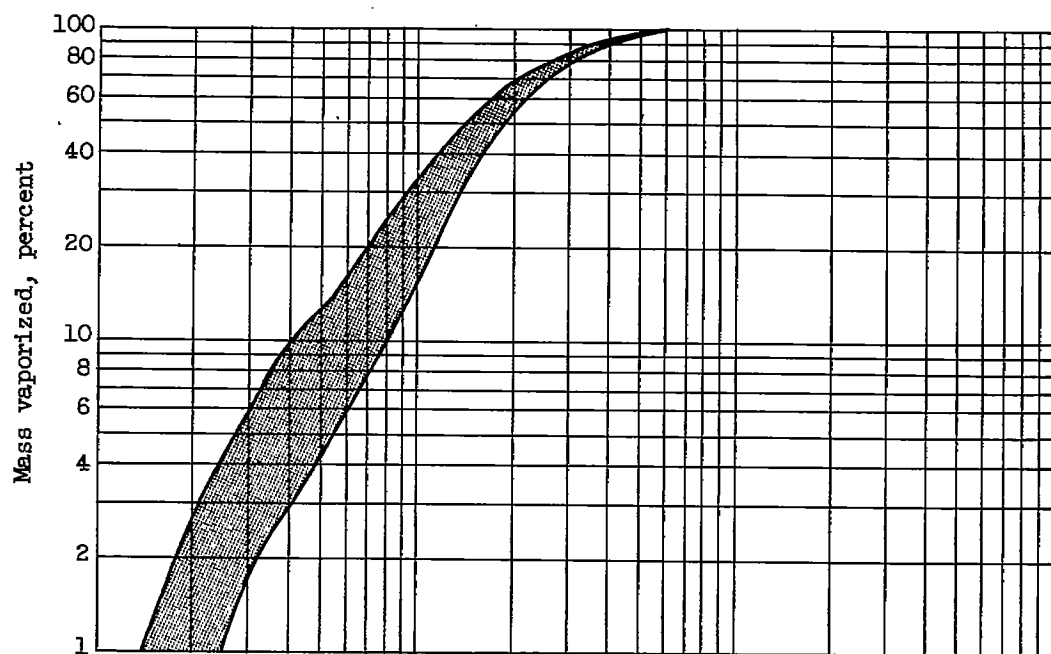Figure 6. - Accumulated drop-mass distribution for five drop-size groups.
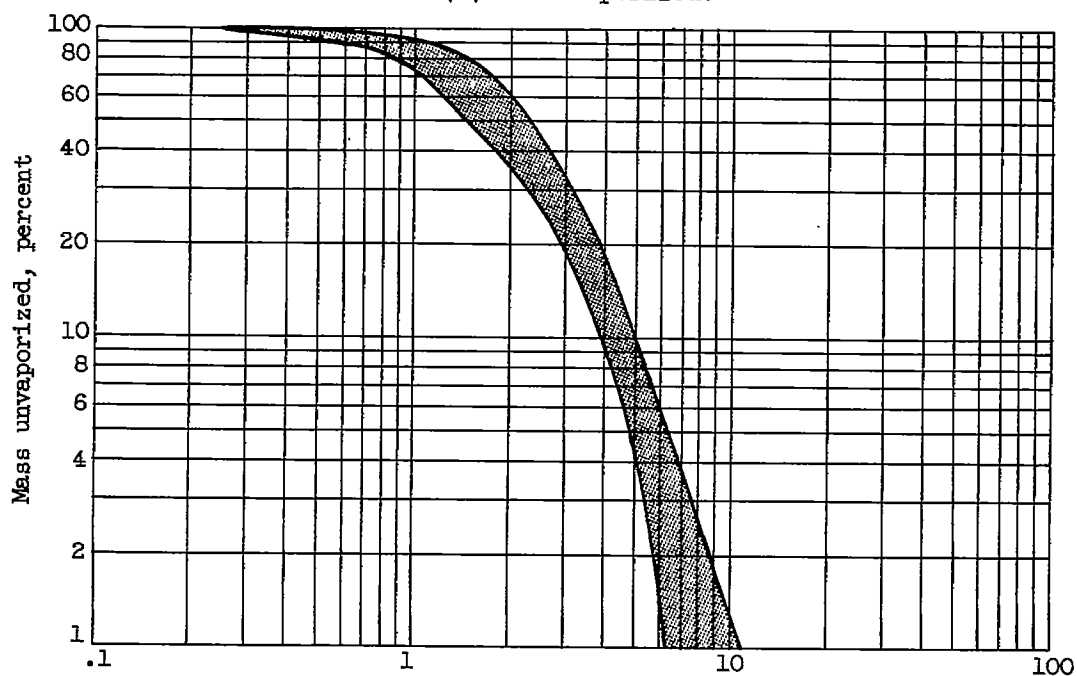
(a) Mass vaporized.

(b) Mass unvaporized.

Figure 7. - Effect of different representation of distribution. Mass-
median-drop radius, 0.003 inch; geometric standard deviation, 1.54;
initial drop temperature, 500° R; initial drop velocity, 1200 inches
per second; final gas velocity, 9600 inches per second; gas tempera-
ture, 5000° R; chamber pressure, 300 pounds per square inch absolute.

(a) Mass vaporized.

(b) Mass unvaporized.

$$\text{Effective length,} \left(\frac{L P^{0.55} u_{\text{fin}}^{0.25} T_{l,0}^{0.25}}{M_{g,M}^{1.45} v_0^{0.75}} \right) 4.15 \times 10^{-5}$$

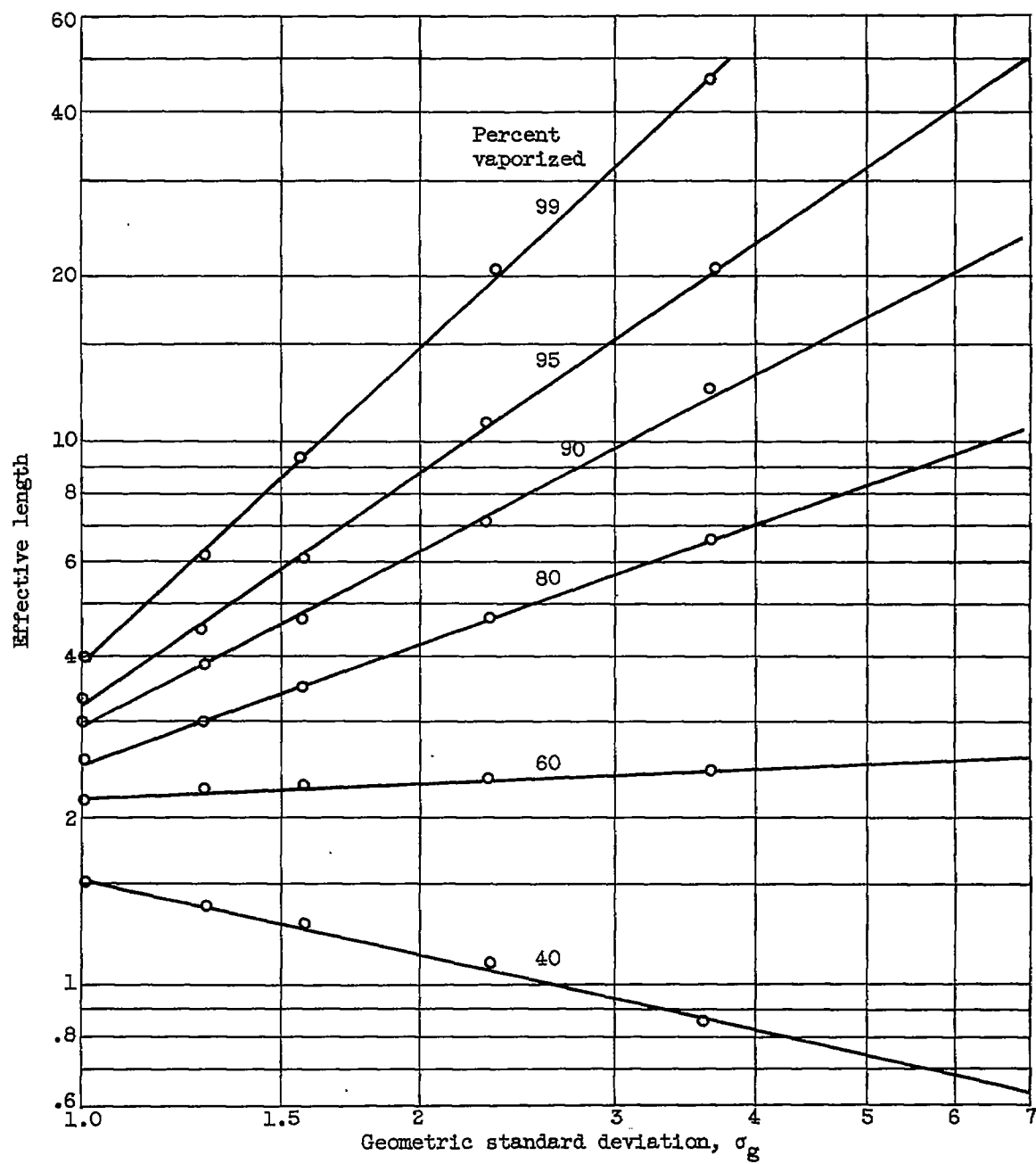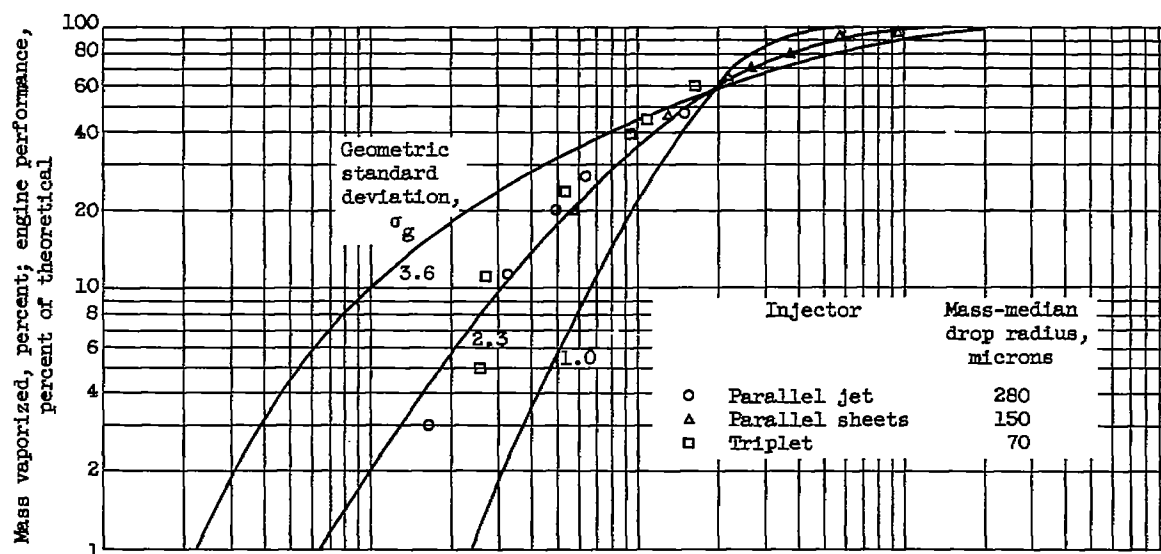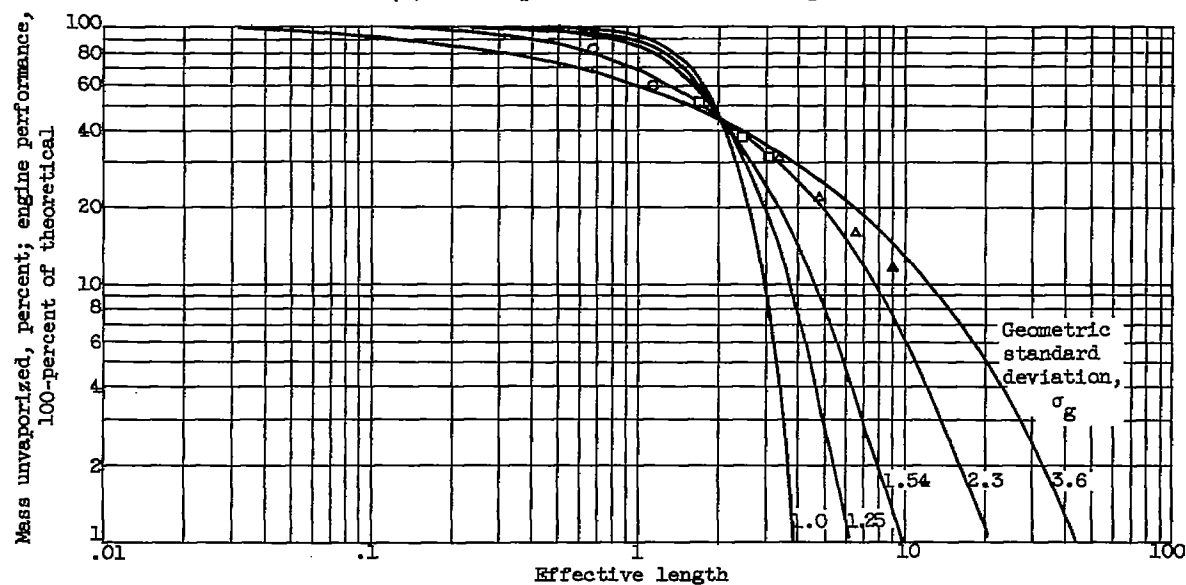Figure 8. – Correlated results for standard deviation of 1.54.

Figure 9. - Effect of geometric standard deviation on effective length for 99, 95, 90, 80, 60, and 40 percent of mass vaporized.

(a) Mass vaporized and theoretical performance.

(b) Mass unvaporized.

Figure 10. - Correlation of results.